MOLECULAR AND CELLULAR BIOLOGY, Aug. 2011, p. 3326–3338 Vol. 31, No. 16
0270-7306/11/$12.00 doi:10.1128/MCB.05718-11

Severe Alterations of Cerebellar Cortical Development after Constitutive Activation of Wnt Signaling in Granule Neuron Precursors▽

Andreas Lorenz,[1]† Markus Deutschmann,[1]† Julia Ahlfeld,[1] Catharina Prix,[1] Arend Koch,[2] Ron Smits,[3] Riccardo Fodde,[4] Hans A. Kretzschmar,[1] and Ulrich Schüller[1]*

Center for Neuropathology, Ludwig Maximilians University, 81377 Munich, Germany[1]; Department of Neuropathology, Charité Universitätsmedizin, 10117 Berlin, Germany[2]; Department of Gastroenterology and Hepatology, Erasmus Medical Center, 3000 CA Rotterdam, The Netherlands[3]; and Department of Pathology, Josephine Nefkens Institute, Erasmus Medical Center, 3000 CA Rotterdam, The Netherlands[4]

Received 30 May 2011/Returned for modification 1 June 2011/Accepted 8 June 2011

The Wnt/β-catenin signaling pathway plays crucial roles in early hindbrain formation, and its constitutive activity is associated with a subset of human medulloblastoma, a malignant childhood tumor of the posterior fossa. However, the precise function of Wnt/β-catenin signaling during cerebellar development is still elusive. We generated *Math1-cre*::*Apc*$^{Fl/Fl}$ mice with a conditional knockout for the *Adenomatosis polyposis coli* (*Apc*) gene that displayed a constitutive activity of Wnt/β-catenin signaling in cerebellar granule neuron precursors. Such mice showed normal survival without any tumor formation but had a significantly smaller cerebellum with a complete disruption of its cortical histoarchitecture. The activation of the Wnt/β-catenin signaling pathway resulted in a severely inhibited proliferation and premature differentiation of cerebellar granule neuron precursors *in vitro* and *in vivo*. Mutant mice hardly developed an internal granular layer, and layering of Purkinje neurons was disorganized. Clinically, these mice presented with significantly impaired motor coordination and ataxia. In summary, we conclude that cerebellar granule neurons essentially require appropriate levels of Wnt signaling to balance their proliferation and differentiation.

The development of the murine cerebellum depends on a well-organized interaction between multiple signaling pathways, which control proliferation, migration, and differentiation of a rather limited number of glial and neuronal cell types. Cerebellar granule neurons outnumber all other types of neurons in the brain, and their proper development crucially determines the overall growth and histoarchitecture of the cerebellum (2). Inappropriate development or loss of granule neurons in mice results in severe cerebellar abnormalities, and several human disease situations are associated with granule cell aplasia (33). Appropriate proliferation of granule neuron precursors proceeds until around postnatal day 15 in mice and 18 months in humans. It is driven mainly by an activated Sonic hedgehog signaling pathway (35), but other mechanisms, such as Igf-2 or Sdf-1 signaling, have also been described to be involved in granule neuron precursor proliferation (12, 18). Constitutive activation of such pathways may, in a pathological situation, result in the formation of medulloblastoma, a frequent malignant brain tumor in children, a subset of which is believed to arise from granule neuron precursors (for a review, see reference 24).

The canonical Wnt/β-catenin signaling pathway has also been implicated both in the early development of the cerebellum and in the biology of medulloblastoma. As a part of this pathway, glycogen synthase kinase 3β (GSK-3β), axin, and adenomatous polyposis coli (Apc) form an intracellular complex that, in the absence of Wnt ligands, promotes degradation of β-catenin, the central mediator of this pathway. Binding of Wnt proteins results in the inactivation of the "destruction complex," β-catenin is translocated to the nucleus, and target gene transcription is activated via TCF/LEF factors. Several studies have shown that functional alterations of this pathway may lead to severe abnormalities in brain development. Deletion of β-catenin in *Nestin*-positive precursors, for instance, results in severely disrupted cortical layering and impressive midline defects with hypoplastic structures of the midbrain/hindbrain region (31). Stabilized β-catenin, in turn, results in enhanced generation of *Nestin*-positive neural precursors and massively enlarged brains (4). In line with this, activating mutations of the β-catenin-encoding *CTNNB1* gene occur in a subset of human medulloblastomas (19, 36), and this distinct subset is further characterized by overexpression of Wnt target genes, such as *DKK1* and *AXIN2* (20, 34).

Adenomatous polyposis coli (Apc) protein, as a part of the intracellular destruction complex, directs the proteolysis of β-catenin and consequently inhibits Wnt signaling. In the colon, Apc therefore acts as a classical tumor suppressor, and mutations of *APC* contribute to the formation of colorectal adenomas and carcinomas (29). Germ line mutations of *APC* cause familial adenomatous polyposis or Turcot's syndrome, which is characterized by both adenomatous polyps of the colorectum and malignant tumors of the central nervous system (CNS), e.g., medulloblastoma (10). In the cerebellum, expression of *Apc* has been reported in granule neurons (3) with a continuous decrease in expression levels during devel-

* Corresponding author. Mailing address: Center for Neuropathology, Ludwig Maximilians University, Feodor-Lynen-Strasse 23, D-81377 Munich, Germany. Phone: 49-89-2180-78114. Fax: 49-89-2180-78037. E-mail: ulrich.schueller@lmu.de.
† These authors contributed equally to this work.
▽ Published ahead of print on 20 June 2011.

opment (17). Also, sporadic medulloblastomas were found to carry *APC* mutations, though in a clearly lower frequency than in colon cancer (14). Despite those tight connections between Wnt signaling, cerebellar development, and formation of medulloblastoma, the functional role of Apc during cerebellar development and its contribution to the proliferation of granule neuron precursors have not been investigated. Homozygous mutations of *Apc* result in embryonic lethality (7), making the analysis of postnatal cerebellar development impossible. Thus, we used the Cre-loxP system to generate conditional *Apc* knockout mice with a deletion of exon 16 within the *Apc* gene. We show here that activation of Wnt signaling through loss of Apc in *Math1*-expressing cerebellar granule neuron precursors resulted in early inhibition of cell proliferation, premature differentiation, and a severely diminished number of granule neurons. This, in turn, resulted in impressive abnormalities of the cerebellar histoarchitecture, including the development of Purkinje neurons. Our results suggest essential roles for Apc during granule neuron precursor proliferation and cerebellar development. A conditional knockout of *Ctnnb1* exon 3, which results in a failure to phosphorylate and degrade β-catenin, uncovered similar changes in *Math1*$^{+}$ granule neurons, suggesting that our results mirror consequences from a constitutive activation of Wnt signaling rather than changes that are specific for the loss of Apc. Together, these aspects of Wnt/β-catenin signaling may have important implications for the understanding of cerebellar disease settings related to granule neuron biology.

MATERIALS AND METHODS

Transgenic mice. The generation of mice carrying a loxP-flanked exon 16 of the *Apc* gene and of mice carrying a loxP-flanked exon 3 of the *Ctnnb1* gene has been described previously (11, 26). *Math1-cre*::*Apc*$^{Fl/Fl}$ mice and *Math1-cre*::*Ctnnb1(ex3)*$^{Fl/+}$ mice were created by crossing mice with floxed alleles to *Math1-cre* mice (32) and kept in the animal care facility under standard conditions. Genotyping was performed by standard PCR using Cre-specific primers (5′-TCCGGGCTGCCACGACCAA-3′ and 5′-GGCGCGGCAACACCATTTT-3′), *Apc*-specific primers (5′-TAGGCACTGGACATAAGGGC-3′ and 5′-GTAACTGTCAAGAATCAATGG-3′), and *Ctnnb1*-specific primers (5′-CGTGGACAATGGCTACTCAA-3′ and 5′-TGTCCAACTCCATCAGGTCA-3′). Intense monitoring of mutant mice included observation of weight and size control, symptoms of slow or impaired movement, and any hints of the development of brain or intestinal tumors.

Clinical testing. To examine the motor performance of mice, we used a RotaRod system (V4.1.1; TSE Systems). The examiner was blinded for the group membership of the tested animals. Initially, mice were trained for 5 days with three trials per day. The RotaRod system accelerated the speed from 0 to 30 rpm over a period of 180 s. On the sixth day, animals were tested with an accelerating speed up to 50 rpm over a period of 300 s. During test trials, each animal was placed individually on the cylinder. Three trials with a cutoff at 10 s were recorded by a computer-based light barrier. The latency between each trial was at least 40 s. To assess the motor coordination and gait, we used a footprint test. To obtain footprints, the hind- and forepaws of the mice were coated with black and green nontoxic paint, respectively. The animals were then allowed to walk along a 40-cm-long, 8-cm-wide tunnel which was placed in a box with 20-cm-high walls on either side. A fresh sheet of white paper was placed on the floor of the runway for each mouse. The footprint patterns were analyzed by measuring the deviation from a proposed path, and the average distance was measured from the left or right front footprint to the hind footprint. When the center of the hind footprint fell on top of the center of the preceding front footprint, a value of zero was recorded. When the footprints did not overlap, the distance between the center points of the footprints was recorded. At least five values were measured from each trial, excluding footprints made at the beginning and end of the runway, where the animal was initiating and finishing its movements, respectively. The mean value of each set was used.

Histology/immunostaining. Standard hematoxylin-and-eosin (H&E) staining was applied to all brain sections. For immunohistochemistry, sections were subjected to heat antigen retrieval at 99°C in 10 mM sodium citrate buffer for 10 min for all antibodies. Staining was performed using the following primary antibodies: anti-Pax6 (1:50; Developmental Studies Hybridoma Bank), anti-E-cadherin (36B5, undiluted; Novocastra), anti-Cmyc (Y69, 1:100; Epitomics), anti-cyclin D1 (RM-9104, 1:100; Labvision), anti-Axin2 (ab32197, 1:200; abcam), anti-Cre (PRB106C, 1:3,000; Covance), anti-Ki-67 (M7249, 1:25; Dako), anti-cleaved caspase 3 (9664, 1:100; Cell Signaling Tech), anti-β-catenin (610154, 1:1,000; BD), anti-BrdU (347580, 1:100; BD), anti-green fluorescent protein [GFP] (sc-8334, 1:50; Santa Cruz), anti-NeuN (MAB377, 1:300; Chemicon), and anti-TuJ1 (MMS435P, 1:500; BABCO). Use of antibodies against BrdU required treatment with 4 N HCl for 10 min and neutralization with 0.1 M sodium borate buffer for 5 min instead of heat retrieval. For the detection of Cmyc, epitope unmasking using TUF Target unmasking fluid (Pan Path) was necessary. Primary antibodies were detected using the avidin-biotin-peroxidase complex (ABC)/3,3′-diaminobenzidine (DAB) method for light microscopy and using fluorescence-coupled secondary antibodies (Alexa Fluor 488 goat anti-rabbit [Molecular Probes], A11008, 1:200, and Alexa Fluor 546 goat anti-mouse [Molecular probes], A11003, 1:200) for double labelings. Cell nuclei were visualized by hematoxylin when using the DAB method and by 4′,6-diamidino-2-phenylindole (DAPI) when using fluorescence-labeled antibodies.

Cell culture. Cerebellar granule neuron precursor cultures were generated as described previously (16). Briefly, cerebella of postnatal day 7 (P7) pups were taken out and prepared in Hanks buffered saline solution (HBSS) (Gibco) with added glucose. Meninges and plexus tissue were carefully removed. Dissociation of pooled cerebella was triggered by trypsin-EDTA-DNase. For the experiments shown in Fig. 5, HBSS was replaced by culture medium containing Dulbecco's modified Eagle medium (DMEM)-F12 (Gibco), 25 mM KCl, N2 supplement (Gibco), penicillin-streptomycin (Pen-strep), and 10% fetal calf serum (FCS) (Sigma) after centrifugation, cells were plated at a concentration of 3 million/ml in poly-L-ornithine (Sigma)-precoated wells and incubated at 37°C for 6 to 12 h to recover. Then, medium was changed to serum-free culture medium containing Shh (R&D systems) at a concentration of 0.6 μg/ml. For the experiments shown in Fig. 8B, cells were cultured under serum-free conditions from the beginning with phosphate-buffered saline (PBS) as a control, Shh (0.6 μg/ml; R&D systems), Shh and Igf2 (200 ng/ml; R&D systems), or Shh and Sdf1a (1 μg/ml). After 24 h, cells were transduced with filtered virus supernatant (as described below) for 2 h, followed by another 24 h of incubation in serum-free medium plus PBS as a control, Shh, Shh and Igf2, or Shh and Sdf1a. Cells were pulsed with BrdU 2 h prior to fixation with 4% paraformaldehyde.

Production of *IRES-GFP* and *Cre-IRES-GFP* virus was carried out as previously published (16). Briefly, 293 packaging cells (Invitrogen) were grown in DMEM–10% FCS–Pen-strep–300 μg/ml G418 and transfected with 10 μg of each virus construct, as well as *vsv-g* and *gag-pol* plasmids, using the Fugene 6 transfection reagent (Roche). Virus collection medium (without G418) was collected every 24 h for three consecutive days, pooled, and stored at −80°C until use.

Nucleic acid extraction and PCR analyses. Genomic DNA from primary cultured murine granule neuron precursors was isolated using the peqGOLD tissue DNA minikit (Peqlab), following the manufacturer's instructions. Genotyping was performed using *Apc*-specific primer 1 (5′-AACTTCTGAGTATGATGGAGG-3′), primer 2 (5′-TAGGCACTGGACATAAGGGC-3′), and primer 3 (5′-GTAACTGTCAAGAATCAATGG-3′). Primers to detect sequences in exon 16 were 5′-TTCATACCTCCCAGGACGAC-3′ and 5′-AGGGTTTCATTTGGCCTCTT-3′. Total RNA from cell cultures and from tissues was extracted using the TRIzol reagent (Invitrogen). To determine whether RNA was sufficient in concentration and quality to suit further analysis, the NanoDrop system was deployed. For reverse transcription, the SuperScript III First-Strand kit (Invitrogen) was applied according to the manufacturer's protocol. Reverse transcription-PCR (RT-PCR) was performed using the LightCycler 480 System (Roche) and the SBYR green detection format. Due to its consistent expression in murine granule neuron precursors, the *beta-2-Microglubolin* (*B2m*) gene was used as a housekeeping control. The following primers were used: *B2m*, 5′-CCTGGTCTTTCTGGTGCTTG-3′ and 5′-TATGTTCGGCTTCCCATTCT-3′; *Axin2*, 5′-GCGACGCACTGACCGACGAT-3′ and 5′-GCAGCAGGTTCCACAGGCGT-3′; *Shh*, 5′-ACCGGGACCGCAGCAAGTACG-3′ and 5′-CACGCGGTCTCCGGGACGTAAGT-3′; *Sdf1a*, 5′-TGGACGCCAAGGTCGTCGC-3′ and 5′-ACCGGCAGGGGCATCGGTAG-3′; *Igf2*, 5′-TGCTGCATCGCTGCTTACGGC-3′ and 5′-CGACGGTTGGCACGGCTTGAA-3′. For each primer set, postamplification melting curves were analyzed with the LightCycler 480 software to verify the specific amplification of the expected PCR product.

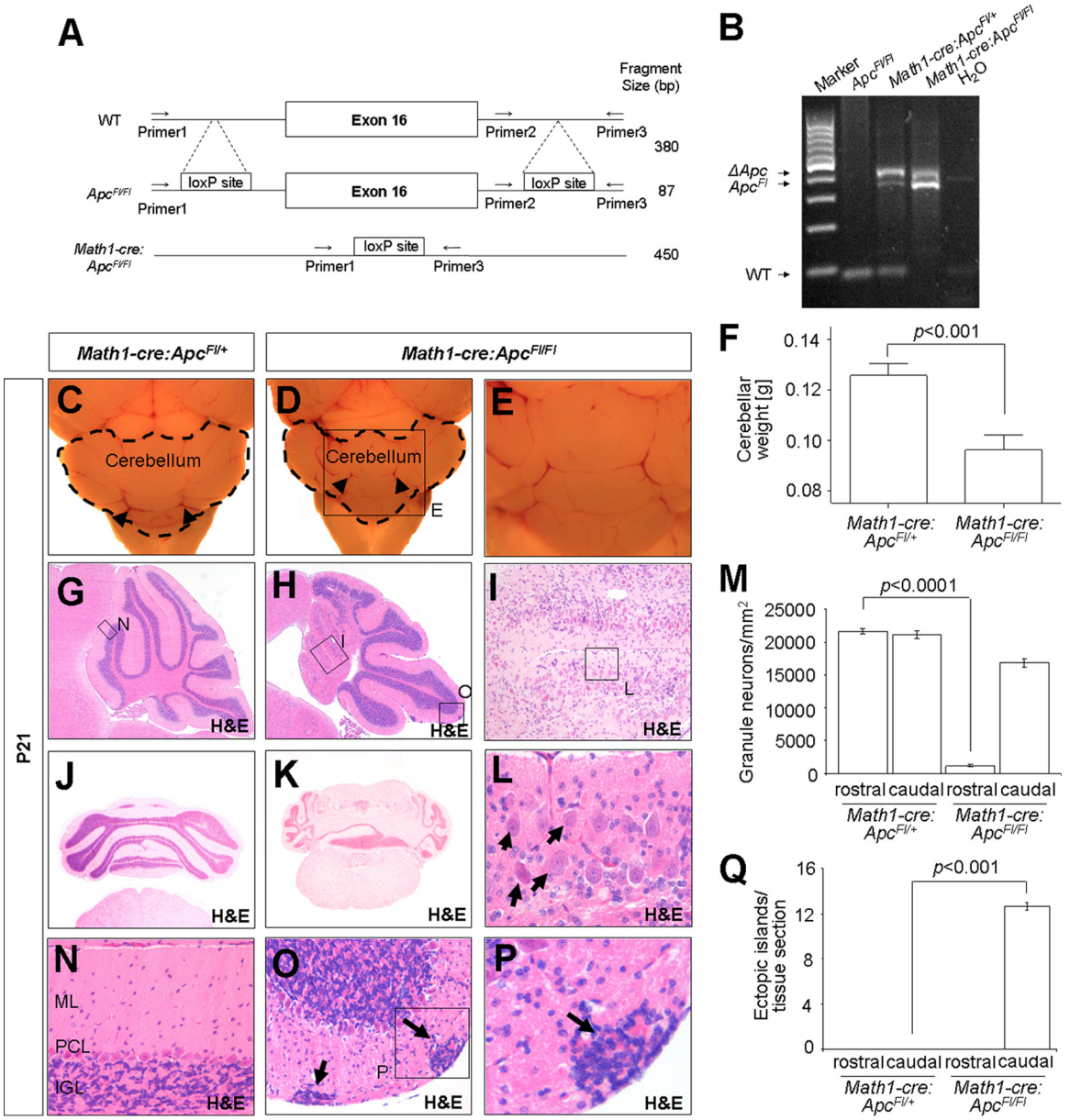

FIG. 1. *Math1-cre*::$Apc^{Fl/Fl}$ cerebella displayed severe histomorphological abnormalities. The scheme shows the *Apc* wild-type (WT) allele, as well as the *Apc* allele with loxP sites before and after exposition to Cre recombinase (A). PCR of isolated cerebellar DNA from P7 mice was carried out using all three primers indicated in panel A and showed a band for the floxed allele (380 bp) and for the recombined allele (450 bp) in *Math1-cre*::$Apc^{Fl/Fl}$ and *Math1-cre*::$Apc^{Fl/+}$ mice but not in the wild-type situation (B). In the wild-type situation, primers 2 and 3 amplified an 87-bp fragment, while the DNA fragment between primers 1 and 3 was not amplified due to its large size. Size and weight of P21 *Math1-cre*::$Apc^{Fl/Fl}$ cerebella ($n = 6$) were largely diminished compared to those for controls ($n = 4$; $P < 0.001$, Student's t test). All values were normalized to total brain weight (C to F). Arrowheads in panels C and D delineate corresponding anatomic landmarks. H&E histology revealed a dramatic depletion of granule neurons and a severely disrupted cortical architecture in rostral parts of *Math1-cre*::$Apc^{Fl/Fl}$ cerebella compared to findings for controls both in sagittal (G to M and L to N) and in horizontal sections (J and K). Note the failure of Purkinje cells to form the typical monolayer in cerebella with Apc-deficient granule cells (arrows in panel L). Hypomorphic caudal areas revealed clusters of granule cells that failed to migrate inwardly (O to Q, arrows). IGL, internal granular layer; ML, molecular layer; PCL, Purkinje cell layer; WM, white matter. Enlarged views of boxed areas in panels D, G, H, I, and O are presented in other panels, as indicated.

Quantifications and statistics. Analysis of phenotypes from conditional knockout mice was performed for at least three mice of each genotype that were all taken from different litters. For quantifications, the number of granule cells per mm external granular layer (EGL) and the percentage of β-catenin- and Ki-67-positive granule cells were determined in three randomly selected locations for three cerebella of each genotype. This was done for the anterior and posterior part of each cerebellum, using the fissure as an arbitrary border between anterior and posterior. In cerebella of p21 mice, granule cells per mm^2 internal granular layer (IGL) were counted. For statistical analysis, the Student t test was used for the evaluation of granule cells per area, whereas the Fisher exact test was used for the assessment of the percentage of β-catenin- and Ki-67 positive cells. For LightCycler assessment, all experiments were done with three mice per genotype, each in triplicate, and statistical analysis was performed using the REST (Relative Expression Software Tool) calculator software program.

Proliferative activity in virus-treated granule neuron precursor cultures was measured in at least three independent culture preparations with three wells of a 24-well plate and at least 300 GFP^+ cells counted in each well of each condition in each preparation. The accumulation of nuclear β-catenin was assessed by counting more than 500 cells, with at least 150 cells in each count. For the experiment shown in Fig. 8, a minimum of 300 cells were counted per condition. Results were analyzed using the Fisher exact test, and P values of <0.05 were considered significant. All obtained results, including those from clinical testing of the mice, were analyzed using the Prism4 software program (GraphPad).

RESULTS

In order to investigate the function of Apc and Wnt/β-catenin signaling in cerebellar granule neuron precursors, we took advantage of the Cre-loxP system and generated conditional knockout mice with a deletion of Apc in granule neuron precursors. To this end, we used *Math1-cre* mice with specific expression of functional Cre recombinase in granule neurons (32). In these mice, the function of Cre recombinase is first detected at embryonic day 12.5 (E12.5) in granule cell precursors giving rise to granule cells that predominantly populate the anterior lobes of the adult cerebellum and later in those populating more caudal lobes, until labeling of all granule cell precursors is complete by E17 (23). Such mice were intercrossed with $Apc^{Fl/Fl}$ mice, which carried loxP sites flanking exon 16 of the *Apc* gene, including the mutational cluster region (26, 30). Successful recombination of exon 16 was demonstrated by PCR and electrophoresis of cerebellar DNA from postnatal day 7 (P7) control and mutant mice (Fig. 1A and B).

Hypoplastic cerebella, loss of granule neurons, and impaired migration due to Apc deficiency. Compared to the situation in control *Math1-cre*::$Apc^{Fl/+}$ mice (Fig. 1C), macroscopic analysis of adult *Math1-cre*::$Apc^{Fl/Fl}$ cerebella displayed dramatic anatomical abnormalities, which were detectable by an irregular blood vessel pattern as well as a severely diminished size of the cerebellum (Fig. 1D and E). *Math1-cre*::$Apc^{Fl/Fl}$ mice ($n = 4$) showed a 23.5% reduction of the cerebellar weight compared to *Math1-cre*::$Apc^{Fl/+}$ mice ($n = 6$; all values were normalized to total brain weight; $P < 0.001$) (Fig. 1F). As seen on H&E stains of sagittal and horizontal sections from adult (P21) control and *Math1-cre*::$Apc^{Fl/Fl}$ cerebella, the reduction in size and weight was explained by a dramatic loss of granule cells, mainly in rostral parts where Math1-cre activity has been described to occur first (23) (Fig. 1G to M). High-power magnifications of rostral lobes of adult *Math1-cre*::$Apc^{Fl/Fl}$ cerebella demonstrated diffusely distributed Purkinje cells, which failed to establish the typical monolayer and which were located close to the cerebellar white matter due to the lack of a proper internal granule cell layer (Fig. 1L, arrows). While granule neurons were barely detectable in rostral parts of *Math1-cre*::$Apc^{Fl/Fl}$ cerebella, caudal parts included ectopic islands of uniformly shaped remnants in superficial parts of the molecular layer (Fig. 1N to P). As displayed in Fig. 1Q and O, these islands were not found in control mice. Immunohistochemistry revealed that cells within these islands did not express nuclear β-catenin (Fig. 2B, arrows), and PCR analysis of microdissected islands confirmed the presence of *Apc* exon 16 sequences which should be deleted after successful homozygous recombination (data not shown). We therefore concluded that the failure of these cells to migrate inward was most likely a secondary effect rather than a consequence of Wnt activity. In order to see whether these cells would represent proliferating progenitors, we assessed the proliferative activity of these cells by analysis of Ki-67 expression and found that all cells within such clusters had left the cell cycle (Fig. 2D). Furthermore, strong expression of Pax6 and NeuN in these cells suggested that they represented mature granule neurons (Fig. 2F and H). In summary, layering and migration of both mutant and wild-type neurons were disturbed in *Math1-cre*::$Apc^{Fl/Fl}$ mice, which in turn resulted in dramatic alterations in the cerebellar histoarchitecture.

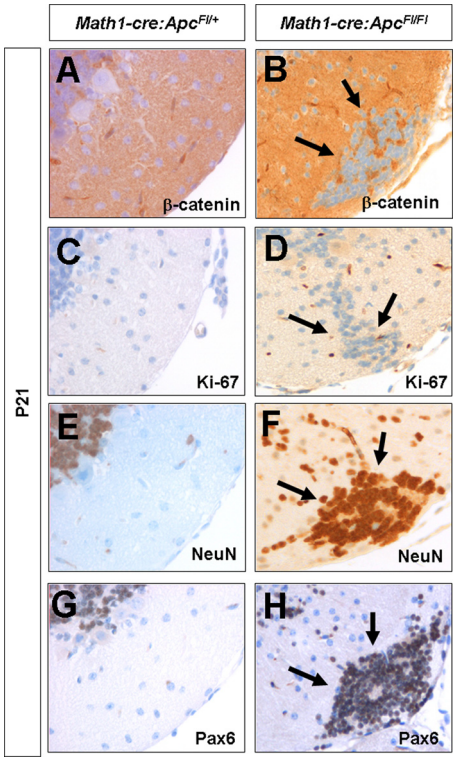

FIG. 2. Characterization of ectopic cell clusters in the molecular layer of *Apc*-deficient cerebella. Cells in the molecular layer of P21 *Math1-cre*::$Apc^{Fl/+}$ cerebella did not express nuclear β-catenin (A), Ki-67 (C), NeuN (E), or Pax6 (G). Similarly, ectopic cell clusters in *Math1-cre*::$Apc^{Fl/Fl}$ cerebella (arrows) did not accumulate β-catenin in cell nuclei (B) (arrows). Furthermore, they did not express Ki-67 (D) (arrows). However, strong expression of NeuN (F) (arrows) and Pax6 (H, arrows) indicated granule neuron identity.

Wnt activation and loss of granule neurons in mice with Math1-driven deficiency of Apc starts around birth. In order to identify the time point of Wnt activation and possible functional consequences in *Math1-cre*::$Apc^{Fl/Fl}$ cerebella, we first looked at cerebella from E16.5. However, H&E-stained sagittal sections of *Math1-cre*::$Apc^{Fl/+}$ and *Math1-cre*::$Apc^{Fl/Fl}$ cerebella did not reveal any differences between the two genotypes at this point (Fig. 3A and C). In particular, no significant differences could be observed regarding the number of granule neurons per mm EGL (Fig. 3Q). Although Cre expression was already detectable at E16.5 (Fig. 3B and D), expression of the β-catenin protein was absent from granule cell nuclei and Axin2 was absent completely in *Math1-cre*::$Apc^{Fl/+}$ (Fig. 3E

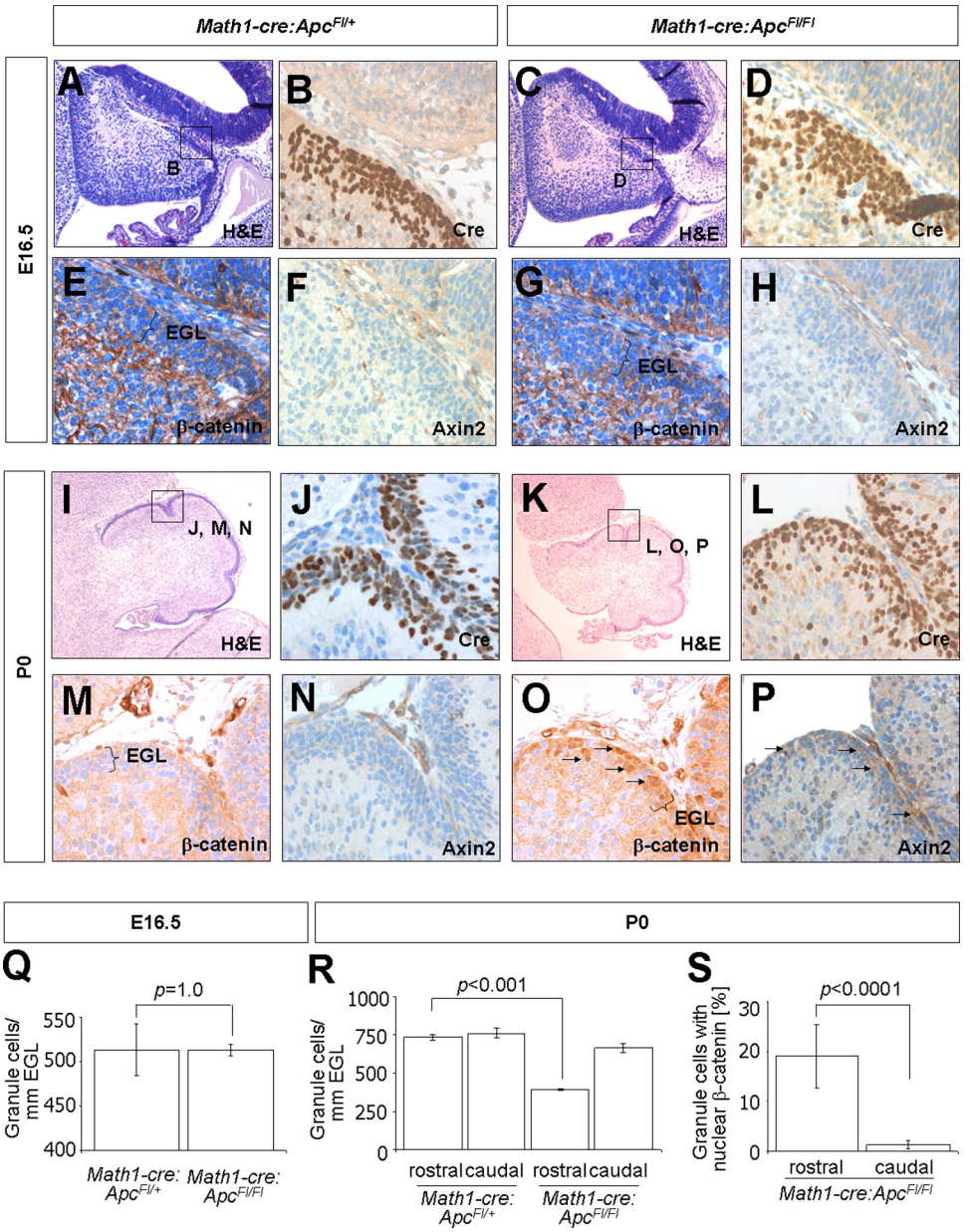

FIG. 3. Constitutive Wnt signaling in granule neuron precursors of *Math1-cre*::$Apc^{Fl/Fl}$ mice was first visible at P0. At E16.5, H&E stainings did not reveal any morphological differences between cerebella of *Math1-cre*::$Apc^{Fl/+}$ and *Math1-cre*::$Apc^{Fl/Fl}$ mice (A, C, and Q). Although Cre recombinase was strongly expressed in cerebellar granule neuron precursors at this age (B and D), Wnt signaling was not active yet, as demonstrated by a failure to detect expression of nuclear β-catenin (E and G) and Axin2 (F and H). However, at P0, the number of granule neuron precursors was significantly diminished in *Math1-cre*::$Apc^{Fl/Fl}$ mice (I, K, and R) ($P < 0.001$), both Cre and β-catenin were found in the nuclei of Apc-deficient granule neurons (J, L, M, O, and S), and Axin2 was upregulated in the EGL of *Math1-cre*::$Apc^{Fl/Fl}$ mice (N and P). All images are taken from sagittal sections. EGL, external granular layer. Enlarged views of boxed areas in panels A, C, I, and K are presented in other panels, as indicated.

and F) and in *Math1-cre*::$Apc^{Fl/Fl}$ (Fig. 3G and H) mice. This indicated that the Wnt signaling pathway was not active yet (e.g., in consequence of Apc loss; see the introduction). Looking at the number of granule neurons at P0, however, did for the first time reveal significant differences between controls (Fig. 3I) and conditional knockout mice (Fig. 3K). While 733 granule cells per mm EGL were visible in rostral parts of control mice, only 393 cells were counted in *Math1-cre*::$Apc^{Fl/Fl}$ mice (Fig. 3R) ($P < 0.001$). No significant differences were seen in caudal parts (Fig. 3R). At P0, Cre expression (Fig. 3J and L) was detectable along with the proof of nuclear β-catenin and Axin2 in *Math1-cre*::$Apc^{Fl/Fl}$ (Fig. 3O, P, and S) mice but not in control mice (Fig. 3M, N, and S). This indicated that Wnt signaling was active at this point, similar to the situation in several types of cancer, including colon cancer (27) and medulloblastoma (5), where β-catenin is detectable in tumor cell nuclei. No nuclear β-catenin was detected outside the EGL of *Math1-cre*::$Apc^{Fl/Fl}$ mice. As a next step, further

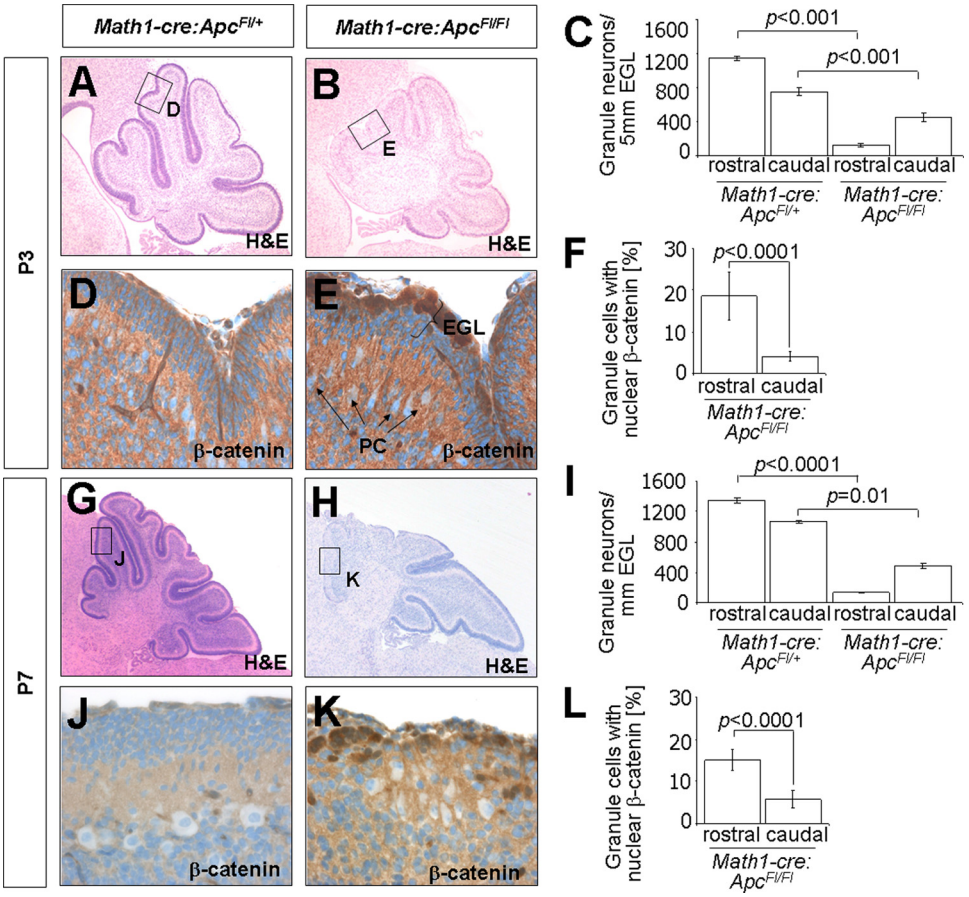

FIG. 4. Severe morphological alterations at P3 and P7 after constitutive Wnt activation in cerebellar granule neuron precursors. From P3 on, consequences of activated Wnt signaling in the EGL were clearly visible on H&E stainings (sagittal sections [A and B]). While control animals exhibited a thick EGL consisting of proliferating granule neuron precursors, *Math1-cre*::*Apc*$^{Fl/Fl}$ mice had only single granule neurons in the EGL. These changes were very clear in rostral parts but were still significant in caudal areas (C). Expression of β-catenin was membranous in control mice (D) but nuclear in almost 20% of granule neurons in rostral parts of Apc-deficient cerebella (E and F). At P7, cerebellar foliation was hardly visible on H&E sections of *Math1-cre*::*Apc*$^{Fl/Fl}$ cerebella (H) compared to findings for control mice (G). The number of granule cells was significantly reduced (I), and nuclear β-catenin was still prominent in Apc-deficient granule cells (K and L). EGL, external granular layer; PC, Purkinje cells. Enlarged views of boxed areas in panels A, B, G, and H are presented in other panels, as indicated.

analyses were performed on older mice in order to see how the observed changes at P0 would develop over time. At P3, the *Math1-cre*::*Apc*$^{Fl/Fl}$ cerebella were already smaller than those of littermate controls, and the number of granule neurons was significantly reduced in both rostral and caudal parts (Fig. 4A to C). Compared to 4% in controls, almost 20% of all EGL cells in conditional knockout animals displayed a nuclear accumulation of β-catenin (Fig. 4D to F) ($P < 0.0001$). At P7, a stage that is normally characterized by maximal proliferation of granule neuron precursors in superficial parts of the premature cerebellar cortex, the foliation of rostral parts of the cerebellum was almost completely absent in *Math1-cre*::*Apc*$^{Fl/Fl}$ mice (Fig. 4G and H), again due to a significant loss of granule neurons (Fig. 4I). Similar to the situation at P3, remaining granule neurons in the external granular layer showed a nuclear accumulation of β-catenin which was present in significantly more cells with Apc deficiency (Fig. 4K) than in control granule cells (Fig. 4J and L).

Wnt activation in cerebellar granule neuron precursors inhibits proliferation and enhances differentiation. Having observed that loss of Apc in granule neuron precursors resulted in Wnt activation and in a significant reduction of granule neurons, we examined the impact of Wnt signaling on the proliferation and apoptosis of cerebellar granule neuron precursors. As expected due to missing Wnt activity (Fig. 3), we did not detect any differences regarding expression of Ki-67 or cleaved caspase 3 in cerebella of controls (Fig. 5A, B, and E) and *Math1-cre*::*Apc*$^{Fl/Fl}$ mice (Fig. 5C to E) at E16.5. However, at P0, P3, and P7, the fraction of granule neuron precursors expressing Ki-67 was significantly reduced in *Math1-cre*::*Apc*$^{Fl/Fl}$ mice (Fig. 5H, J, M, O, R, and T) compared to that in *Math1-cre*::*Apc*$^{Fl+l}$ mice Fig. 5F, J, K, O, P, T). This was true in rostral and in caudal areas. Enhanced numbers of apoptotic cells were not observed at any developmental stage (Fig. 5B, D, G, I, L, N, Q, and S).

Although the function of *Math1-cre* has previously been described to differ in rostral and caudal parts of the developing cerebellum (see above) (23), our findings raised the possibility that an activation of Wnt signaling has region-dependent effects during cerebellar development. We therefore asked whether granule cell precursor proliferation

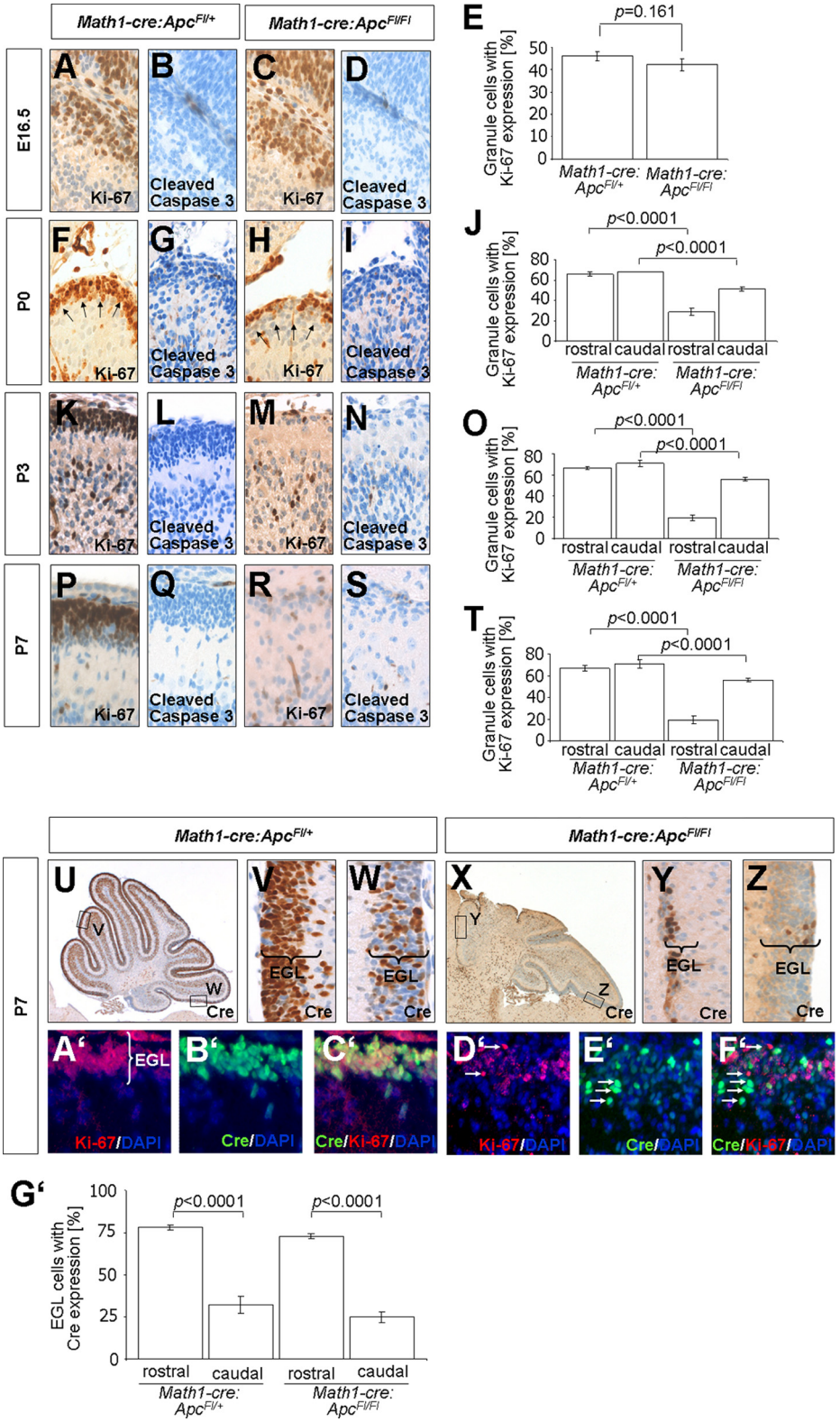

FIG. 5. Reduced proliferation and enhanced differentiation in Apc-deficient granule neurons. While the fraction of Ki-67-positive granule neuron precursors was similar in control mice and *Math1-cre*::$Apc^{Fl/Fl}$ animals at E16.5 (A, C, and E), significant changes appeared at P0 (F, H, and J) and were still present at P3 (K, M, and O) and P7 (P, R, and T). These changes were prominent in rostral parts but were also detectable in caudal parts of the cerebellum. An altered number of apoptotic granule cells that expressed cleaved caspase 3 was not detected at any time point analyzed (B, D, G, I, L, N, Q, and S). Regional differences of Cre expression in *Math1-cre* cerebella were obvious, since approximately 75% of granule neuron precursors expressed Cre in rostral parts of *Math1-cre*::$Apc^{Fl/+}$ and *Math1-cre*::$Apc^{Fl/Fl}$ cerebella but only about 25% did so in caudal parts (U to Z and G'). Interestingly, Cre-expressing granule neuron precursors coexpressed Ki-67 in control animals (A' to C') but not in *Math1-cre*::$Apc^{Fl/Fl}$ cerebella (D' to F'). EGL, external granular layer; PC, Purkinje cells. Enlarged views of boxed areas in panels U and X are presented in other panels, as indicated.

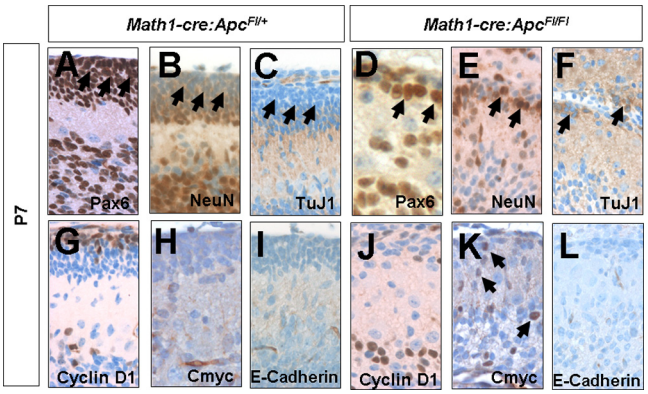

FIG. 6. Granule neuron identity and enhanced differentiation of superficially located mutant granule neurons. Granule neuron identity and differentiation were suggested by expression of Pax6 (A and D, arrows), NeuN (B and E, arrows), and TuJ1 (C and F, arrows). Compared to control cells (G), most of the Apc-deficient cells did not express cyclin D1 (J). Cmyc was not expressed in control cells (H) but was expressed in mutant cells (K, arrows), and E-cadherin was expressed neither in control (I) nor in Apc-deficient (L) cells. All images are taken from representative areas of the rostral cerebellum.

was directly related to the expression of Cre recombinase rather than to the anatomical localization. As shown by immunolabeling using antibodies against Cre recombinase for both *Math1-cre*::$Apc^{Fl/+}$ mice (Fig. 5U to W) and *Math1-cre*::$Apc^{Fl/Fl}$ mice (Fig. 5X to Z), the vast majority of granule neuron precursors in rostral parts of the cerebellum expressed high levels of Cre, but clearly fewer cells were stained within the EGL of caudal parts (Fig. 5G') ($P < 0.0001$). This mirrored the previously described phenomenon of region-specific *Math1* promoter activity (23, 28) and suggested that regional differences in phenotype penetrance resulted from incomplete recombination in caudal parts of the cerebellum rather than from different susceptibilities to Wnt signaling. We further performed colocalization studies with antibodies against Cre recombinase and Ki-67. While granule neuron precursors that showed an activation of the *Math1* promoter proliferated and expressed Ki-67 in control mice (Fig. 5A' to C'), expression of Cre and that of Ki-67 were mutually exclusive in *Math1-cre*::$Apc^{Fl/Fl}$ cerebella (arrows in Fig. 5D' to F'). This was true for rostral and caudal parts of the cerebellum. We therefore concluded that constitutive Wnt signaling cell-autonomously inhibited proliferation of cerebellar granule neuron precursors and prevented regular expansion of premature granule neurons in all parts of the cerebellum, yet to various degrees.

Next, we aimed to see whether Apc deficiency in cerebellar granule neuron precursors would go along with a change in lineage identity or differentiation. We analyzed the expression of Pax6, NeuN, and TuJ1 in control and Apc-deficient granule neurons (Fig. 6A to F). Pax6, which is known as a marker of the granule cell lineage (6), was expressed by all cells within the EGL of both control and *Math1-cre*::$Apc^{Fl/Fl}$ cerebella (arrows in Fig. 6A and D). NeuN and TuJ1 normally show weak or no expression in outer parts of the EGL (arrows in Fig. 6B and C), while protein expression becomes strong as soon as granule cells migrate into deeper parts of the EGL, where differentiation is initiated. However, both markers were strongly expressed in superficially located cells of *Math1-cre*::$Apc^{Fl/Fl}$ cerebella (arrows in Fig. 6E and F), indicating that Wnt activity through loss of Apc did not change lineage identity but induced premature neuronal differentiation in cerebellar granule cells. We further asked whether cyclin D1 and Cmyc, encoded by two well-described target genes of Wnt signaling, were expressed in Apc-deficient granule neurons. While cyclin D1 is expressed by superficial neuronal precursors in the EGL of P7 control cells (Fig. 6G), no such strong expression could be detected in *Math1-cre*::$Apc^{Fl/Fl}$ cerebella (Fig. 6J). Conversely, Cmyc was not detected in controls (Fig. 6H), while several superficially located cells expressed Cmyc in conditional knockout mice (Fig. 6K). To see whether expression of E-cadherin was involved in the described consequences of Wnt activation in granule neurons, we used antibodies against E-cadherin, but we did not find significant upregulations (Fig. 6I and L).

As a next step, we aimed to investigate whether we could confirm the above-described results of reduced granule neuron proliferation due to constitutive Wnt activity by *in vitro* experiments. We therefore cultured primary cerebellar granule neuron precursors from P7 $Apc^{Fl/Fl}$ pups and acutely deleted Apc by transducing cells with either *IRES-GFP* or *Cre-IRES-GFP* viruses. All measurements were done 24 h after virus application. First, genomic DNA was extracted from cultured granule neuron precursors, and PCR confirmed correct recombination and excision of *Apc* exon 16 after *Cre-IRES-GFP* virus application (Fig. 7A and B). Second, colabeling of GFP and β-catenin was performed to demonstrate membranous β-catenin staining in successfully transduced, GFP^+ control cells (Fig. 7C to E), and nuclear β-catenin staining was used as an indicator of Wnt activity in successfully transduced GFP^+ cells with Cre-mediated loss of Apc (arrows in Fig. 7F to I). In addition, Wnt activity was measured quantitatively by determining the relative expression of *Axin2*, a well-known target gene of Wnt signaling (22). As shown in Fig. 7J, expression of *Axin2* was upregulated almost 2.5-fold in mRNA from $Apc^{Fl/Fl}$ granule neuron precursors transduced with *Cre-IRES-GFP* viruses compared to results for cells transduced with *IRES-GFP* viruses ($P = 0.012$, Student's *t* test). Finally, incorporation of BrdU was measured to estimate the proliferate activity of granule neuron precursors. As shown in Fig. 7K to Q, incorporation of BrdU was reduced from 55.2 ± 4.9% in cells that were transduced with *IRES-GFP* viruses to 36.4 ± 4.8% in cells that were transduced with *Cre-IRES-GFP* control viruses ($P = 0.015$, Student's *t* test). We therefore concluded that the acute loss of Apc in cultured cerebellar granule neuron precursors caused an immediate activation of Wnt signaling and a significant inhibition of Sonic hedgehog (Shh)-induced proliferation.

Proliferation of cerebellar granule neuron precursors is regulated not only by Shh but also by Igf2 and Sdf1a (12, 18). It therefore appeared possible that reduced proliferation of cerebellar granule neuron precursors after Wnt activation was caused by reduced activity of Igf2 or Sdf1a. With this idea in mind, we first used RT-PCR analyses to determine the expression levels of *Shh*, *Igf2*, and *Sdf1a* in cerebella from P0 control and *Math1-cre*::$Apc^{Fl/Fl}$ mice. In addition, levels of *Axin2* were measured to control for upregulated Wnt signaling pathways in these mice. As shown in Fig. 8A, levels of *Axin2* were about

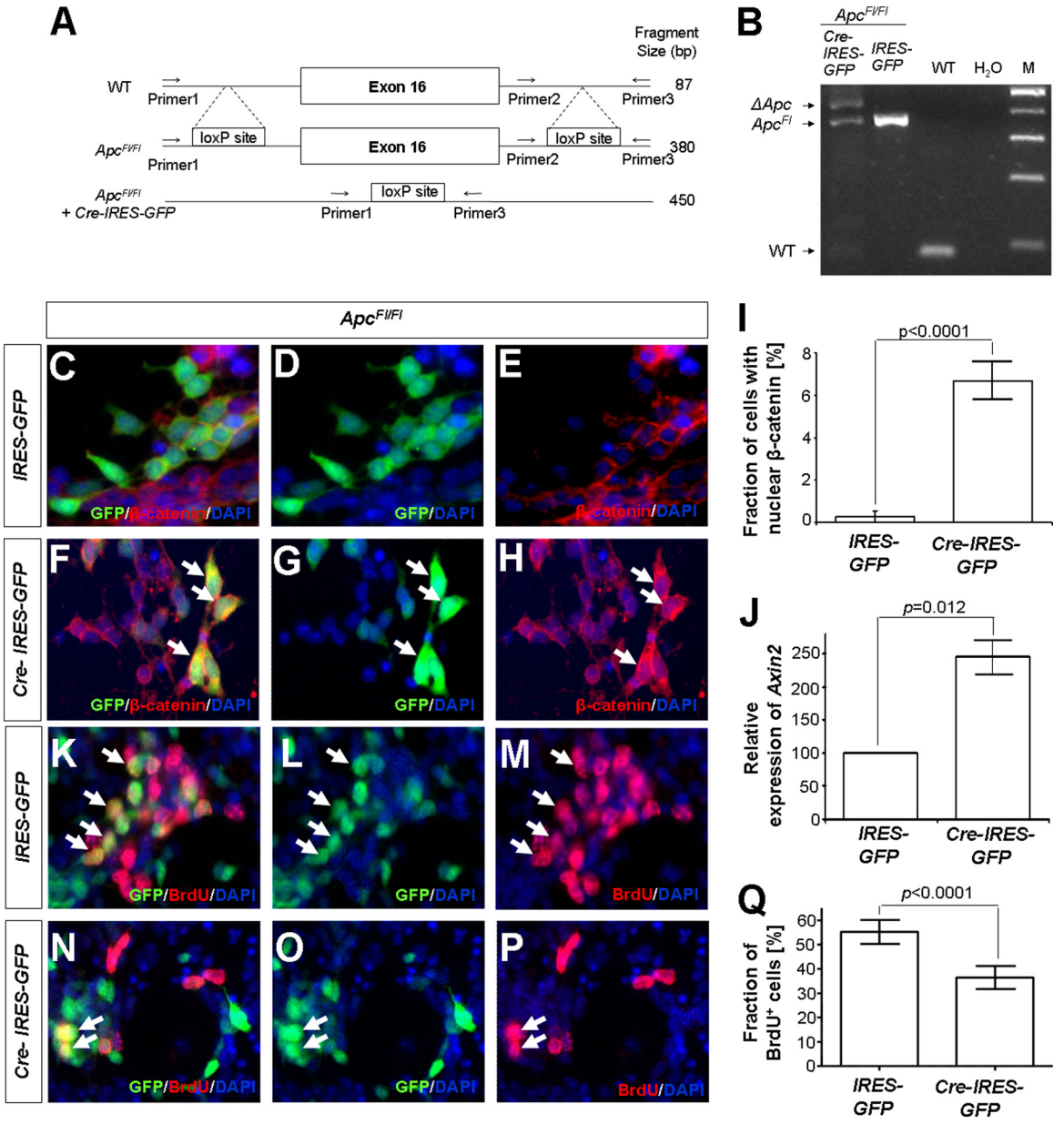

FIG. 7. Acute loss of Apc resulted in significantly reduced proliferation of primary cultured cerebellar granule neuron precursors. The scheme shows the *Apc* wild-type (WT) allele, as well as the *Apc* allele with loxP sites before and after exposition to Cre recombinase (A). PCR of isolated DNA from $Apc^{Fl/Fl}$ granule neuron precursors that were cultured at P7 and transduced with either *IRES-GFP* or *Cre-IRES-GFP* virus was carried out using all three indicated primers. The gel shows successful recombination resulting in a fragment of 450 bp after treatment with *Cre-IRES-GFP* virus (B). Primers flanking the right loxP insertion site produced a fragment of 380 bp in both *Cre-IRES-GFP*- and *IRES-GFP*-treated cultures from $Apc^{Fl/Fl}$ mice but not in WT animals, where only 87 bp were amplified (B). Note that the DNA fragment between primers 1 and 3 was not amplified in unrecombined cells due to its large size. Granule neuron precursor cells were cultured from $Apc^{Fl/Fl}$ mice at P7 and transduced with either *Cre-IRES-GFP* or *IRES-GFP* virus. Staining with antibodies against β-catenin featured nuclear accumulation in only 0.35% of cells transduced with *IRES-GFP* (C to E and I) but in 6.5% of cultured cells treated with *Cre-IRES-GFP* (G and H, arrows; I; $P < 0.0001$, Fisher exact test). Quantitative RT-PCR revealed a significant increase in the transcriptional activity of the Wnt target gene *Axin2* in cultures from $Apc^{Fl/Fl}$ mice treated with *Cre-IRES-GFP* virus (J) ($P = 0.012$, Student's *t* test). Statistical analysis of subsequent immunocytochemical stainings using antibodies against BrdU revealed significantly fewer proliferating cells under conditions with *Cre-IRES-GFP* virus treatment (N to Q) than under control conditions (K to M and Q; $P = 0.015$, Student's *t* test). Values in panel Q are shown as means ± SEM from 3 independent experiments.

2-fold upregulated, as expected ($P < 0.001$), but neither *Shh*, *Igf2*, nor *Sdf1a* was downregulated. In fact, *Igf2* was almost 2-fold upregulated ($P < 0.05$), consistent with reports on *Igf2* being a target gene of Wnt signaling (1). As a second experiment to check whether Igf2 and Sdf1a would still function in Wnt-activated granule neurons, we treated primary cultured granule neuron precursors with and without Wnt activity with Shh, Shh plus Igf2, or Shh plus Sdf1a. However, Wnt activity did not have any impact on the synergistic effect of Igf2 or Sdf1a on Shh-induced proliferation of granule cell precursors

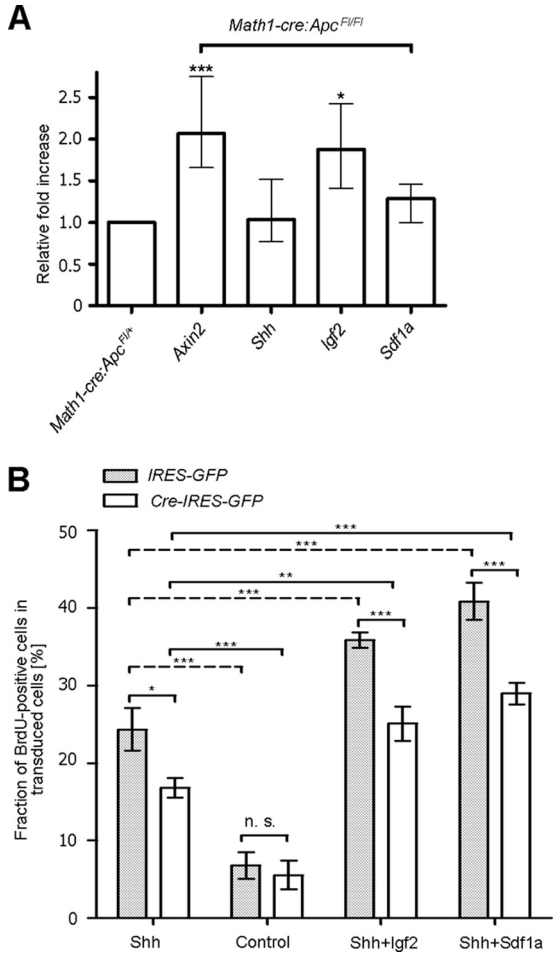

FIG. 8. Impact of activated Wnt signaling on expression and function of Shh, Sdf1a, and Igf2. Both *Axin2* and *Igf2* mRNA are about 2-fold upregulated in *Math1-cre*::$Apc^{Fl/Fl}$ cerebella compared to findings for *Math1-cre*::$Apc^{Fl/+}$ cerebella. No significant changes were detected with respect to *Shh* and *Sdf1a* expression levels. All tissue samples were from P0 mice (A). Granule neuron precursor cells from P7 $Apc^{Fl/Fl}$ mice were cultured and treated either with PBS (control), with Shh, with Shh plus Igf2, or with Shh plus Sdf1a. Both under control conditions (filled bars; cells transduced with *IRES-GFP* Viruses) and in cells with an activated Wnt signaling pathway (empty bars; cells transduced with *Cre-IRES-GFP* Viruses), Igf2 and Sdf1a acted synergistically on Shh-induced proliferation of granule neuron precursors (B). *, $P < 0.05$; **, $P < 0.01$; ***, $P < 0.001$.

(Fig. 8B). We therefore concluded that the Wnt-associated inhibition of granule cell precursor proliferation was not mediated by an impairment of Igf2 or Sdf1a function.

Conditional stabilization of β-catenin in granule neuron precursors has effects similar to those of loss of Apc. In order to determine whether the morphological alterations observed in *Math1-cre*::$Apc^{Fl/Fl}$ mice represented specific consequences of an Apc deficiency or whether they represented general alterations that occurred due to an activated Wnt signaling in the cerebellum, we crossed *Math1-cre* mice to mice with a conditional allele with loxP sites flanking exon 3 of the *Ctnnb1* gene (11). Loss of this exon causes a failure of β-catenin to be phosphorylated and degraded by the "destruction complex" (see the introduction). Subsequent translocation of β-catenin to, and an accumulation in, the cell nucleus ultimately results in target gene activation and gain of function. Analysis of H&E stainings from sagittal sections of early postnatal (P0, Fig. 9A to C; P7, Fig. 9D to K) and adult cerebella (P21, Fig. 9L and M) of *Math1-cre* mice and *Math1-cre*::*Ctnnb1(ex3)*$^{Fl/+}$ mice revealed that both the loss of granule neurons in rostral parts of the cerebellum with high Cre activity and the impaired migration of granule cells in caudal parts of the cerebellum with low levels of Wnt activity were similar to the findings observed for *Math1-cre*::$Apc^{Fl/Fl}$ mice. In particular, proliferation was similarly impaired in granule neuron precursors of P7 *Math1-cre*::*Ctnnb1(ex3)*$^{Fl/+}$ mice, as revealed by immunohistochemistry using antibodies against Ki-67 (Fig. 9H, J, and K). We therefore concluded that the described phenotypic alterations mirrored consequences of an activated Wnt/β-catenin signaling pathway in cerebellar granule neuron precursors, independent of how this activation was initiated.

Clinical deficits but no tumor development in adult *Math1-cre*::$Apc^{Fl/Fl}$ mice. Apc acts as a classic tumor suppressor and is involved in both the generation of colon cancer and medulloblastoma (see the introduction). We asked whether, in the long term, mice with a *Math1*-driven deletion of Apc would develop tumors and observed *Math1-cre*::$Apc^{Fl/Fl}$ mice ($n = 20$) for a period of up to 6 months. None of the mice died or showed any histological sign of tumor development in the CNS or the colon (data not shown), but all of the tested mutant mice displayed clinical abnormalities. Motor and balance coordination was tested in a RotaRod apparatus and, after five training days, *Math1-cre*::$Apc^{Fl/Fl}$ mice performed significantly worse than control mice ($P = 0.01$, Student's t test) (Fig. 10A). Similar results were obtained from a gait test, which was performed to assess ataxia and impairment of fine control of movements. As measured by the distance between forepaw and hindpaw and by the deviation from a proposed path, *Math1-cre*::$Apc^{Fl/Fl}$ mice again performed significantly worse than wild-type mice ($P = 0.005$ and $P = 0.02$, respectively) (Fig. 10B).

DISCUSSION

The first studies that indicated relevant roles of Wnt signaling for the development of the cerebellum appeared almost 20 years ago (25). However, mechanistic details on how Wnt signaling and single pathway components contribute to the control of proliferation and differentiation in granule neuron precursors of the cerebellum are not yet understood. In this study, we provide evidence that a physiological regulation of Wnt signaling is essential for the appropriate proliferation and differentiation of cerebellar granule neuron precursors. Our results shed new light on the role of Wnt signaling in the early development of the brain, and they will be crucial for the understanding of the distinct roles that Wnt signaling may play in different cellular compartments.

Wnt signaling during cerebellar development. Apc is well known for its tumor-suppressive roles in various types of cancer, including medulloblastoma, and all of these tumors exhibit features of an activated Wnt signaling pathway. Similarly, a constitutive activation of Wnt signaling during neural development has been reported to cause an expansion of precursor populations and a massively enlarged brain (4). In line with

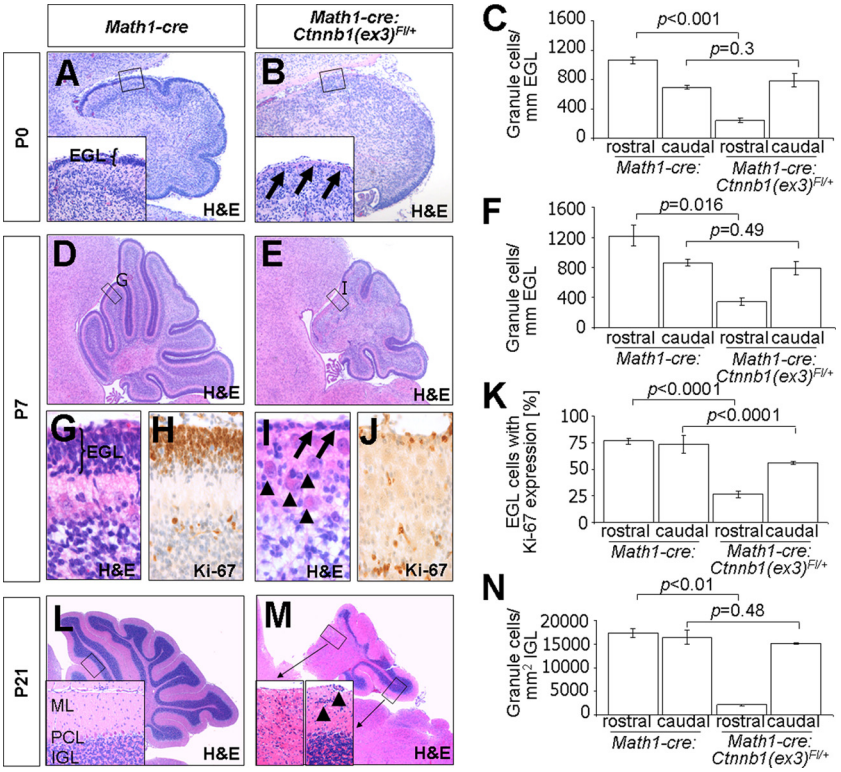

FIG. 9. *Math1-cre*::*Ctnnb1(ex3)*$^{Fl/+}$ cerebella displayed severe histomorphological abnormalities similar to those of cerebella of *Math1-cre*::*Apc*$^{Fl/Fl}$ mice. At P0, the sizes of the cerebella were still comparable between *Math1-cre* (A) and *Math1-cre*::*Ctnnb1(ex3)*$^{Fl/+}$ (B) mice, but the EGL was already thinned out in rostral parts of *Math1-cre*::*Ctnnb1(ex3)*$^{Fl/+}$ cerebella (B, arrows in inset) with significantly fewer granule neurons per mm EGL (C). At P7, the overall size of the mutant cerebellum was reduced (D and E), the EGL was severely diminished in rostral parts of the cerebellum (F, G, and I, arrows), and Purkinje neurons were diffusely distributed within the cerebellar cortex (I, arrowheads). Compared to *Math1-cre* cerebella (H), Ki-67 labeling was restricted to very few cells in the *Math1-cre*::*Ctnnb1(ex3)*$^{Fl/+}$ EGL (J and K). At P21, *Math1-cre*::*Ctnnb1(ex3)*$^{Fl/+}$ cerebella (M) were much smaller than those of controls (L). No granule cell layer was visible in rostral parts of the knockout cerebellum (M), and caudal parts displayed clusters of ectopic granule neurons that were stuck within superficial parts of the molecular layer (M, inset, arrowheads; N). All panels represent stainings from sagittal sections. EGL, external granule cell layer; IGL, internal granular layer; ML, molecular layer; PCL, Purkinje cell layer. Enlarged views of boxed areas in panels D and E are presented in other panels, as indicated.

this, inhibition of Wnt signaling has been linked to an inappropriate proliferation of neural precursor cells and severe brain malformations in several studies (4, 25, 31). These results appear to be in contrast to our data from the current study, which propose that Apc is required for the proliferation of cerebellar granule neuron precursors. We found that loss of Apc leads to an activation of Wnt signaling, and this in turn blocks precursor cell proliferation. However, it is important to note at this point that all of the above-mentioned studies either used conventional knockout mice, transgenes expressed under the control of *Nestin* promoter sequences, or conditional knockout mice with expression of Cre recombinase that is driven by *Nestin* promoter sequences. Since we used *Math1* promoter sequences to delete Apc and activate Wnt signaling, it appears possible that Wnt activation at different time points of development has different or even opposing effects. Indeed, this hypothesis is supported by recent findings that described a conditional inactivation of Apc in proliferating cerebral cortical cells and their descendants (15). As opposed to the enhanced progenitor cell proliferation in the *Nestin*Δ*90*β-*cat* mice (4), Ivaniutsin and coworkers described a significant decrease in the proliferation of cerebral precursor cells when using an *Emx1-cre* line to conditionally knock out Apc (15). *Emx1-cre*::*Apc*$^{Fl/Fl}$ mice show a perfect activation of Wnt signaling, but this does not occur before E10.5, a time point long after activation of the *Nestin* promoter used by Chenn and Walsh (4). Furthermore, *in vitro* activation of Wnt signaling in E11.5 neural precursors by expression of Wnt7a also resulted in enhanced neuronal differentiation (13). Similarly, previous data indicate that the *Math1* promoter which we used is activated no earlier that E12.5 in granule neuron precursors with a rostral-to-caudal sequence (23), and we ourselves did not see any nuclear accumulation of the β-catenin protein before P0 (Fig. 2).

Implications for brain tumor development. The molecular characterization of Turcot's syndrome approximately 15 years ago first implied a causative relation between alterations in the *APC* gene and the formation of medulloblastoma, a malignant childhood tumor that arises in the posterior fossa (10). As revealed in the course of time, up to 20% of human medulloblastomas are characterized by a nuclear accumulation of β-catenin and a distinct gene expression profile that indicates the activation of Wnt signaling (9, 20). Many of these tumors carry mutations of Wnt signaling pathway components (e.g., *CTNNB1* or *APC*), and it appears plausible that a pathological activation of Wnt signaling, for instance caused by *APC* muta-

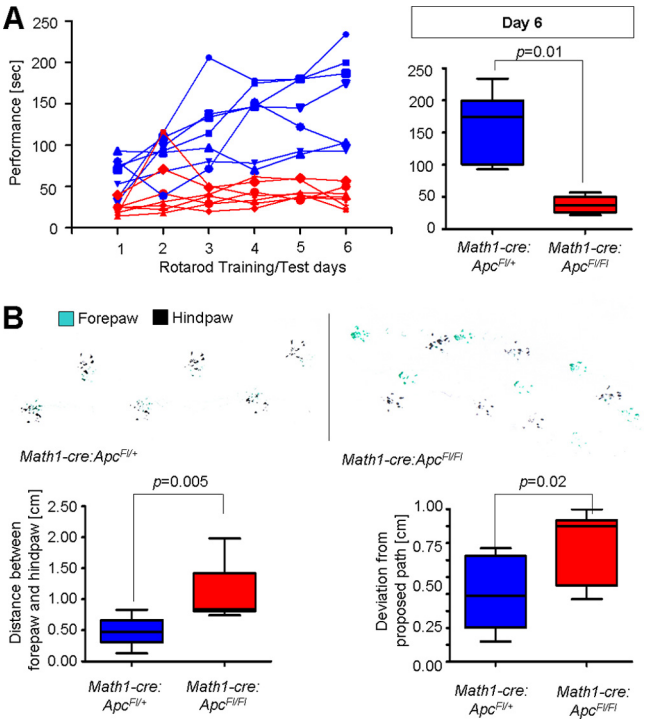

FIG. 10. Adult *Math1-cre*::$Apc^{Fl/Fl}$ mice showed severe clinical deficits. Control mice ($n = 7$) performed significantly better than *Math1-cre*::$Apc^{Fl/Fl}$ mice ($n = 7$) on a Rotarod (A). The left panel displays performance of all 5 training days and of the testing on day 6. Results for control mice are shown in blue; results for *Math1-cre*::$Apc^{Fl/Fl}$ mice are shown in red. The right panel demonstrates the significance of test differences on day 6 ($P = 0.01$). Gait analysis using green ink for forepaws and black ink for hindpaws revealed clearly visible differences between control and *Math1-cre*::$Apc^{Fl/Fl}$ mice (B). The distance between forepaw and hindpaw, as well as the deviation from a proposed path, was significantly higher in *Math1-cre*::$Apc^{Fl/Fl}$ mice than in control mice ($P = 0.005$ and $P = 0.02$, respectively). All results are shown in box-whisker plots with bars delineating the median, boxes the second and third quartile, and whiskers the minimum and maximum of all values. Significance of differences between two groups was analyzed using Student's *t* test.

tions, may result in the formation of medulloblastoma. The most convincing evidence for this theory is represented by Turcot's syndrome (see above), but researchers have failed until now to exactly model this situation in mice. Neither $Apc^{+/min}$ mice nor any other mouse model for Wnt-associated cancer has ever been reported to develop brain tumors. Even the expression of a stabilized form of β-catenin in cerebellar granule neurons under the control of a murine *PrP* promoter fragment does not result in the formation of medulloblastoma (21). Similarly to the work by Kratz et al (21), we have shown here that a conditional knockout of Apc in *Math1*-expressing granule neuron precursors did result in an accumulation of β-catenin in neuronal nuclei but not in the formation of medulloblastoma. In fact, we observed a dramatic inhibition of cell proliferation and a severely reduced size of the cerebellar cortex. This was not described by the previous study and may be caused by the fact that we used *Math1* instead of *PrP* promoter sequences to activate Wnt signaling.

Taken together, our results suggest that Wnt-associated medulloblastomas do not stem from granule neuron precursors but from other neural precursors, which express neither *PrP* nor *Math1*. Indeed, very recent results published by Gibson and colleagues indicated that Wnt-associated medulloblastoma may arise from neuronal precursors in the dorsal brainstem (8). Interestingly, these authors also used *Math1-cre*::*Ctnnb1(ex3)*$^{Fl/+}$ mice to search for possible formation of Wnt-associated tumors in the cerebellar EGL. In line with our findings, they showed less proliferation in cultured granule neuron precursors transduced with *Ctnnb1* mutants than was found with controls (see supplemental Fig. 8P for reference 8), but unfortunately, they did not describe respective findings *in vivo* and only stressed that they did not find tumors in more than 20 mice examined.

ACKNOWLEDGMENTS

We thank Michael Schmidt and Silvia Occhionero for excellent technical assistance. We further acknowledge Stefanie Ohlemeyer and Mehdi Shakarami for animal husbandry. *Ctnnb1(ex3)*$^{Fl/+}$ mice were a generous gift from Mark Taketo (University of Tokyo, Tokyo, Japan).

U.S. is supported by German Cancer Aid (Max Eder Junior research program), by the Wilhelm-Sander-Stiftung, by the Fritz-Thyssen-Stiftung, and by the Friedrich-Baur-Stiftung.

REFERENCES

1. **Adesina, A. M., et al.** 2009. Gene expression profiling reveals signatures characterizing histologic subtypes of hepatoblastoma and global deregulation in cell growth and survival pathways. Hum. Pathol. **40:**843–853.
2. **Altmann, J., and S. A. Bayer.** 1997. Development of the cerebellar system in relation to its evolution, structure and functions. CRC Press, New York, NY.
3. **Bhat, R. V., J. M. Baraban, R. C. Johnson, B. A. Eipper, and R. E. Mains.** 1994. High levels of expression of the tumor-suppressor gene Apc During development of the rat central-nervous-system. J. Neurosci. **14:**3059–3071.
4. **Chenn, A., and C. A. Walsh.** 2002. Regulation of cerebral cortical size by control of cell cycle exit in neural precursors. Science **297:**365–369.
5. **Eberhart, C. G., T. Tihan, and P. C. Burger.** 2000. Nuclear localization and mutation of beta-catenin in medulloblastomas. J. Neuropathol. Exp. Neurol. **59:**333–337.
6. **Engelkamp, D., P. Rashbass, A. Seawright, and H. V. van.** 1999. Role of Pax6 in development of the cerebellar system. Development **126:**3585–3596.
7. **Fodde, R., et al.** 1994. A targeted chain-termination mutation in the mouse apc gene results in multiple intestinal tumors. Proc. Natl. Acad. Sci. U. S. A. **91:**8969–8973.
8. **Gibson, P., et al.** 2010. Subtypes of medulloblastoma have distinct developmental origins. Nature **468:**1095–1099.
9. **Gilbertson, R. J.** 2004. Medulloblastoma: signalling a change in treatment. Lancet Oncol. **5:**209–218.
10. **Hamilton, S. R., et al.** 1995. The molecular basis of Turcot's syndrome. N. Engl. J. Med. **332:**839–847.
11. **Harada, N., et al.** 1999. Intestinal polyposis in mice with a dominant stable mutation of the beta-catenin gene. EMBO J. **18:**5931–5942.
12. **Hartmann, W., et al.** 2005. Insulin-like growth factor II is involved in the proliferation control of medulloblastoma and its cerebellar precursor cells. Am. J. Pathol. **166:**1153–1162.
13. **Hirabayashi, Y., et al.** 2004. The Wnt/beta-catenin pathway directs neuronal differentiation of cortical neural precursor cells. Development **131:**2791–2801.
14. **Huang, H. T., et al.** 2000. APC mutations in sporadic medulloblastomas. Am. J. Pathol. **156:**433–437.
15. **Ivaniutsin, U., Y. J. Chen, J. O. Mason, D. J. Price, and T. Pratt.** 2009. Adenomatous polyposis coli is required for early events in the normal growth and differentiation of the developing cerebral cortex. Neural Dev. **4:**3.
16. **Kenney, A. M., and D. H. Rowitch.** 2000. Sonic hedgehog promotes G1 cyclin expression and sustained cell cycle progression in mammalian neuronal precursors. Mol. Cell. Biol. **20:**9055–9067.
17. **Kho, A. T., et al.** 2004. Conserved mechanisms across development and tumorigenesis revealed by a mouse development perspective of human cancers. Genes Dev. **18:**629–640.
18. **Klein, R. S., et al.** 2001. SDF-1 alpha induces chemotaxis and enhances Sonic hedgehog-induced proliferation of cerebellar granule cells. Development **128:**1971–1981.
19. **Koch, A., et al.** 2001. Somatic mutations of WNT/wingless signaling pathway components in primitive neuroectodermal tumors. Int. J. Cancer **93:**445–449.
20. **Kool, M., et al.** 2008. Integrated genomics identifies five medulloblastoma

subtypes with distinct genetic profiles, pathway signatures and clinicopathological features. PLoS One **3:**e3088.
21. **Kratz, J. E., et al.** 2002. Expression of stabilized beta-catenin in differentiated neurons of transgenic mice does not result in tumor formation. BMC Cancer **2:**33.
22. **Lustig, B., et al.** 2002. Negative feedback loop of Wnt signaling through upregulation of conductin/Axin2 in colorectal and liver tumors. Mol. Cell. Biol. **22:**1184–1193.
23. **Machold, R., and G. Fishell.** 2005. Math1 is expressed in temporally discrete pools of cerebellar rhombic-lip neural progenitors. Neuron **48:**17–24.
24. **Marino, S.** 2005. Medulloblastoma: developmental mechanisms out of control. Trends Mol. Med. **11:**17–22.
25. **McMahon, A. P., and A. Bradley.** 1990. The Wnt-1 (Int-1) protooncogene is required for development of a large region of the mouse brain. Cell **62:**1073–1085.
26. **Miclea, R. L., et al.** 2009. Adenomatous polyposis coli-mediated control of beta-catenin is essential for both chondrogenic and osteogenic differentiation of skeletal precursors. BMC Dev. Biol. **9:**26.
27. **Morin, P. J., et al.** 1997. Activation of beta-catenin-Tcf signaling in colon cancer by mutations in beta-catenin or APC. Science **275:**1787–1790.
28. **Pan, N., I. Jahan, J. E. Lee, and B. Fritzsch.** 2009. Defects in the cerebella of conditional Neurod1 null mice correlate with effective Tg(Atoh1-cre) recombination and granule cell requirements for Neurod1 for differentiation. Cell Tissue Res. **337:**407–428.
29. **Powell, S. M., et al.** 1992. Apc mutations occur early during colorectal tumorigenesis. Nature **359:**235–237.
30. **Robanus-Maandag, E. C., et al.** 2010. A new conditional Apc-mutant mouse model for colorectal cancer. Carcinogenesis **31:**946–952.
31. **Schüller, U., and D. H. Rowitch.** 2007. Beta-catenin function is required for cerebellar morphogenesis. Brain Res. **1140:**161–169.
32. **Schüller, U., et al.** 2007. Forkhead transcription factor FoxM1 regulates mitotic entry and prevents spindle defects in cerebellar granule neuron precursors. Mol. Cell. Biol. **27:**8259–8270.
33. **ten Donkelaar, H. J., M. Lammens, P. Wesseling, H. O. Thijssen, and W. O. Renier.** 2003. Development and developmental disorders of the human cerebellum. J. Neurol. **250:**1025–1036.
34. **Thompson, M. C., et al.** 2006. Genomics identifies medulloblastoma subgroups that are enriched for specific genetic alterations. J. Clin. Oncol. **24:**1924–1931.
35. **Wechsler-Reya, R., and M. P. Scott.** 2001. The developmental biology of brain tumors. Annu. Rev. Neurosci. **24:**385–428.
36. **Zurawel, R. H., S. A. Chiappa, C. Allen, and C. Raffel.** 1998. Sporadic medulloblastomas contain oncogenic beta-catenin mutations. Cancer Res. **58:**896–899.